BJU International

Ex vivo fluorescence confocal microscopy: the first application for real-time pathological examination of prostatic tissue

Stefano Puliatti*, Laura Bertoni†, Giacomo M. Pirola*, Paola Azzoni†, Luigi Bevilacqua*, Ahmed Eissa*‡, Ahmed Elsherbiny*‡, Maria C. Sighinolfi*, Johanna Chester†, Shaniko Kaleci†, Bernardo Rocco*, Salvatore Micali*, Ilaria Bagni§, Luca Reggiani Bonetti§, Antonino Maiorana§, Josep Malvehy¶, Caterina Longo**††, Rodolfo Montironi‡‡, Giampaolo Bianchi*† and Giovanni Pellacani†††

*Department of Urology, †Department of Surgical, Medical, Dental and Morphological Sciences with Interest Transplant, Oncological and Regenerative Medicine, University of Modena and Reggio Emilia, Modena, Italy, ‡Urology Department, Faculty of Medicine, Tanta University, Tanta, Egypt, §Department of Pathology, Ospedale Policlinico e Nuovo Ospedale Civile S. Agostino Estense Modena, University of Modena and Reggio Emilia, Modena, Italy, ¶Melanoma Unit, Dermatology Department, Hospital Clinic, Barcelona, Spain, **Azienda Unit Sanitaria Locale – IRCCS di Reggio Emilia, Centro Oncologico ad Alta Tecnologia Diagnostica- Dermatologia, Reggio Emilia Modena, ††Department of Dermatology, University of Modena and Reggio Emilia, Modena, and ‡‡Department of Pathological Anatomy, Polytechnic University of the Marche Region, School of Medicine, United Hospitals, Ancona, Italy

Objective

To report the first application of *ex vivo* fluorescence confocal microscopy (FCM) - a novel optical technology that is capable of providing fast microscopic imaging of unfixed tissue specimens- in the urological field assessing its diagnostic accuracy for non neoplastic and cancerous prostate tissue (prostatic adenocarcinoma) compared to the 'gold standard' histopathological diagnoses.

Patients and methods

In all, 89 specimens from 13 patients with clinically localised prostate cancer were enrolled into the study. All patients underwent robot-assisted laparoscopic radical prostatectomy with fresh prostatic tissue biopsies taken at the end of each intervention using an 18-G biopsy punch. Specimens were randomly assigned to the three collaborating pathologists for evaluation. Intra- and inter-observer agreement was tested by the means of Cohen's κ. The diagnostic performance was evaluated on receiver operating characteristic curve analysis.

Results

The overall diagnostic agreement between FCM and histopathological diagnoses was substantial with a 91% correct diagnosis (κ = 0.75) and an area under the curve of 0.884 (95% confidence interval 0.840–0.920), 83.33% sensitivity, and 93.53% specificity.

Conclusion

FCM seems to be a promising tool for enhanced specimens' reporting performance, given its simple application and very rapid microscopic image generation (<5 min/specimen). This technique may potentially be used for intraoperative pathological specimens' analysis.

Keywords

fluorescence confocal microscopy, RALP, digital pathology, #Prostate cancer, #PCSM

Introduction

Background

Prostate cancer is the most commonly diagnosed male cancer worldwide [1] and its management is a delicate balance between optimum postoperative functional outcomes and oncological radicalness [2]. Several recent diagnostic and managerial innovations have been introduced, including multiparametric MRI (mpMRI), mpMRI-ultrasonography fusion targeted biopsy, neurovascular bundle-sparing radical prostatectomy (RP) technique, and robot-assisted laparoscopic approach to RP (RALP) [3–5].

However, the 'gold standard' pathological assessment of prostate cancer is still a conventional, time-consuming approach [6]. Moreover, a cancer-free surgical margin is considered a critical part of prostate cancer surgery, as

BJU International © 2019 BJU International | doi:10.1111/bju.14754
Published by John Wiley & Sons Ltd. www.bjui.org

positive surgical margins (PSMs) can be found in up to 38% of patients after RP [1,7]. PSM is one of the major 'surgically controlled' concerns of RP, as it is associated with an increased risk of recurrence, the need for adjuvant therapy, and increased management costs [1,6].

The concept of 'real-time' pathological examinations [6,8,9] initially appeared in the late 1800s, with the first report of the 'intraoperative frozen section' technique in 1895 [10]. After >120 years, this technique is still the gold standard real-time pathological assessment, despite debatable results [6,8,9].

A potential new method of real-time prostate cancer tissue evaluation is *ex vivo* fluorescence confocal microscopy (FCM). FCM provides optical microscopic images of freshly excised tissue in two different modalities; the reflectance mode, based upon different refractive indices of subcellular structures, and the fluorescence mode, using fluorescent agents to increase the contrast within epithelium-stroma of untreated *ex vivo* specimens. It has mainly been applied to the diagnoses of dermatological cancers, such as basal cell and squamous cell carcinomas [11,12]. Preliminary research into FCM as a diagnostic tool for other visceral organ cancers seems promising [13]. Furthermore, it showed to be a promising tool for diagnosis of cutaneous inflammatory skin lesions [14].

Some previously cited FCM technical limitations have recently been overcome through increasing three-fold the field of acquisition and the velocity with which it is acquired, and improving digital staining processing (transforming previous black and white images into coloured images that is able to mimic haematoxylin and eosin [H&E] staining). The advantage of FCM compared to histological examinations is primarily time; the procedure is performed within a few minutes, directly at the patient bedside. Further, the quality of FCM images, produced on a cellular and even nuclear level, have an H&E-like appearance and resolution and the application of FCM evaluation does not compromise tissue for further conventional pathological assessment [15].

Aim of the work

Based upon the benefits of FCM, i.e., faster diagnosis in different surgical settings, we hypothesised that such advantages are transferrable to urology, choosing to investigate firstly prostate cancer due to its widespread diffusion. In the present preliminary analysis, we aimed to explore the feasibility of FCM in the examination of prostatic tissues (diagnostic discrimination of FCM imaging for non-neoplastic and cancerous prostate tissue [prostatic adenocarcinoma] compared to the gold standard histopathological diagnoses). We intentionally chose fresh specimens from RP for the increased probability of the presence of malignant tissue in such samples already diagnosed with prostate cancer.

Patients and methods

Study type and patients recruitment

This single-centre prospective study was approved by the local Ethics Committee (Protocol 0018091/18) and was carried out according to the Declaration of Helsinki. Written informed consent was provided by all participating patients. Consecutive patients undergoing RALP for low-, medium- or high-risk prostate cancer were enrolled. All procedures were carried out by two expert surgeons (G.B., B.R.) with the da Vinci® Surgical System (Intuitive Surgical, Inc., Sunnyvale, CA, USA). Preoperative, intraoperative, pathological and follow-up data were collected and stored in an electronic database.

Study endpoints

The study's primary outcome was to assess the level of agreement between FCM evaluation and histopathological diagnosis of prostatic specimens. Secondary endpoints included the level of agreement for the identification of typical malignancy features at FCM and histopathological evaluation, the level of confidence of digital imaging interpretation, as assessed by the collaborating pathologists, and the assessment of inter-observer reliability.

Biopsy preparation

Using an 18-G biopsy punch, an average of six random prostate biopsies (range four to eight) were freshly acquired at the end of each intervention. Biopsies were immediately treated with a staining process; tissue specimens were completely immersed in acridine orange solution (0.6 mM; Sigma-Aldrich, St. Louis, MO, USA) ®) for 30 s before being rinsed in physiological saline solution to wash off any excess solution. The samples were placed on absorbent paper, and then embedded between two glass slides, fixed with silicon glue. Glass sandwiches were then positioned onto the FCM stage for image acquisition. FCM images were then saved on a dedicated hard disk, according to a patient identification number and intervention date.

Instrument

The FCM VivaScope® 2500M-G4 (MAVIG GmbH, Munich, Germany; Caliber I.D.; Rochester, NY, USA) combines two different lasers that enable tissue examination according to reflectance (785 nm) and fluorescence (488 nm) modalities. The FCM device has a vertical resolution of 4 μm and a maximum examination depth of 200 μm. Increasing the laser power and/or the incubation period of the specimen in the staining solution allows mechanical amplification of the fluorescence and reflectance signals resulting in possible visualisation of deeper structures. Furthermore, as the specimens are glued to glass slides in a sandwich technique, the two sides of the glass sandwich can be examined by the FCM allowing better

evaluation of the deeper side of the specimen. Magnification reaches × 550 and the reconstructed image is a collection of mosaic images (square shaped images of 1024 × 1024 pixels). The maximum total scan area is 25 × 25 mm; however, larger tissues can be examined by cutting it into multiple specimens. The microscope is equipped with a 38× water immersion objective with a numerical aperture of 0.85 [16]. For the present study, the FCM incorporated software, VivaScan® (version 11.0.1140 MAVIG GmbH; Caliber I.D.), VivaBlock® and VivaStack® were used to obtain tissue images. The digital staining modality was used to convert the reflectance and fluorescence greyscale mosaics into colour images. For the present study, a new modality of pixel coloration by self-written ImageJ software (https://imagej.nih.gov/ij/) was applied to the standard digital image approach; [17] each greyscale pixel is converted into a digitally stained image, in which nuclei appear purple and collagen and cytoplasm appear pink. The reflectance and fluorescence brightness in FCM images are inverted to the absorbance-based contrast, as is performed in histopathology imaging. Zoom capabilities enable an enhanced visualisation of cell morphology details.

The staining and imaging processes were completed within 5 min. After the acquisition of FCM images, stained samples were formalin fixed in a biopsy container (Biopsafe ApS; Bygstubben, Denmark) and sent for histopathological evaluation.

Sample examinations

Three pathologists with various levels of expertise (L.R.B., A.M. and R.M.) participated in the study. All acquired FCM images were randomly displayed to collaborating pathologists prior to proceeding to the histopathological diagnosis. The pathologists were instructed to independently identify the presence of four typical malignancy features (atypical glands, enlarged nuclei, prominent nucleoli, and infiltrative pattern of glandular growth) and to differentiate between cancerous and non-neoplastic tissue (FCM evaluation). Furthermore, they were instructed to express their degree of confidence with the digital imaging interpretation (scale ranging from zero to 100).

The prepared prostatic tissue samples were evaluated by the same three pathologists for the presence of the same four typical malignancy features. A final histopathological diagnosis was then made and in case of disagreement between the three pathologists, the histopathological diagnosis reached by the majority was considered final.

Statistical analysis

The Cohen's κ statistic was used to measure the agreement between the FCM and histopathological diagnoses, and for the presence of typical malignancy features identified at FCM and histopathology evaluations, as the variables are binary [18]. Inter-observer agreement was evaluated for FCM evaluation in relation to histopathological diagnosis. The adopted interpretation of agreement includes: a less than chance agreement (κ = 0), slight agreement (κ = 0.01–0.20), fair agreement (κ = 0.21–0.40), moderate agreement (κ = 0.41–0.60), substantial agreement (κ = 0.61–0.80), and almost perfect agreement (κ = 0.81–0.99). Furthermore, the adopted interpretation of reproducibility includes: marginal (κ <0.40), good (κ = 0.40–0.75), and excellent (κ >0.75) [19]. Pearson correlation coefficient was used to measure the correlation between the level of confidence of the pathologists in FCM diagnosis and the gold standard.

Table 1 FCM evaluation of prostatic biopsies compared to histopathological diagnoses, the percentage of correct diagnoses, κ-value and significance for all raters and each operator.

	Histopathological diagnoses		% of correct diagnosis	κ-value	Level of agreement
	Prostatic adenocarcinoma	Non-neoplastic prostate			
FCM evaluation					
All pathologists					
Prostatic acinar adenocarcinoma	55	11	91	0.75***	Substantial
Non-neoplastic prostate	14	187			
Pathologist 1					
Prostatic acinar adenocarcinoma	17	1	92	0.78***	Substantial
Non-neoplastic prostate	6	65			
Pathologist 2					
Prostatic acinar adenocarcinoma	17	1	92	0.78***	Substantial
Non-neoplastic prostate	6	65			
Pathologist 3					
Prostatic acinar adenocarcinoma	21	9	88	0.71***	Substantial
Non-neoplastic prostate	2	57			

FCM evaluation of prostatic biopsies compared to histopathological diagnoses, the percentage of correct diagnoses, k-value and significance for all raters and each operator.
****P < 0.001.*

The diagnostic performance was evaluated on the receiver operating characteristic (ROC) curve and the area under the curve (AUC). A ROC curve describes the relationship between the sensitivity and specificity of a test. The two are inversely related, and the plot is, therefore, a representation of the trade-off between detecting true and false positives. Moreover, a two-way model of interclass correlation (ICC) was used to assess the inter-observer reliability by comparing the variability of different ratings of the same subject to the total variation across all ratings and all subjects. ICC results were interpreted as: poor (<0.5), moderate (0.5–0.74), good (0.75–0.9) and excellent (>0.9) reliability [20].

For all analyses a $P < 0.001$ was considered statistically significant. MedCalc Statistical Software version 14.8.1 (MedCalc Software bvba, Ostend, Belgium; http://www.medcalc.org; 2014) and STATA program version 14 (StataCorp LP, College Station, TX, USA) were used for statistical analyses.

Fig. 1 ROC curve that describes the relationship between the sensitivity and specificity of FCM evaluation and histopathological assessment of all three pathologists.

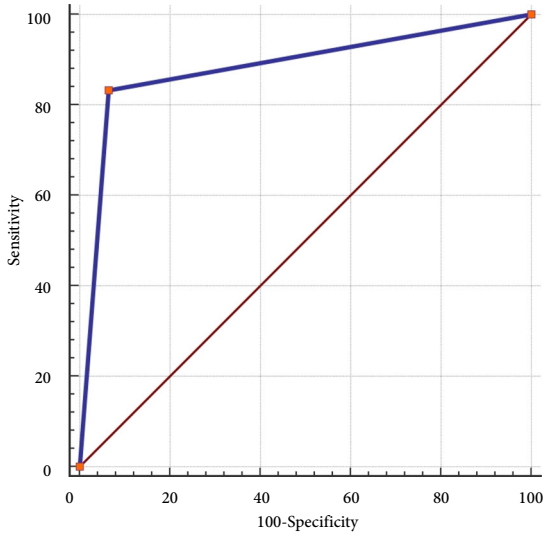

Results

Patient characteristics

A total of 89 biopsies were collected from 13 consecutive patients who underwent RALP at our centre. The mean (SD; range) patient age was 63.8 (7.64; 51–75) years and the mean (SD; range) PSA level was 9.1 (7.65; 3.2–28.0) ng/mL. Clinical staging was T1c and T2c in 84.6% and 15.4%, respectively. The most represented preoperative Gleason Scores were Gleason Score 6 (Gleason Grade Group 1 [GGG1]) in seven patients, Gleason Score 7 (3 + 4) [GGG2] in three patients, Gleason Score 7 (4 + 3) [GGG3] in two patients, and Gleason Score 9 (5 + 4) [GGG 5] in one patient [21]. The median (SD; range) operative time (defined as time from incision to suture) was 175.6 (21.8; 160–215) min. The definitive pathological staging was pT2a, pT2b, pT2c and pT3a in 7.7%, 7.7%, 30.8% and 53.9% of the analysed patients, respectively. Furthermore, the most represented RP Gleason Score was 7 (3 + 4) in six patients followed by Gleason Score 6 in four patients, whilst, Gleason Score 7 (4 + 3), Gleason Score 8 (4 + 4) and Gleason Score 9 (5 + 4) were reported in one patient each.

Primary endpoint

Overall diagnostic agreement between FCM and histopathological diagnoses was substantial with a 91% correct diagnosis ($\kappa = 0.75$) and an AUC of 0.884 (95% CI 0.840–0.920), 83.33% sensitivity, and 93.53% specificity. Data are outlined in Table 1. The relationship between the sensitivity and specificity of overall FCM diagnosis and histopathological diagnosis is shown in Fig. 1. The individual diagnostic agreement was substantial for each pathologist (Table 1).

Secondary endpoints

Table 2 shows the level of agreement for the identification of typical malignancy features at FCM and histopathological evaluation. The Cohen's κ statistic identified the infiltrative pattern of glandular growth as the feature with the highest level of agreement (an almost perfect; 0.83) and an excellent

Table 2 AUC, sensitivity and specificity of the final diagnosis and for the pathological features for all the pathologists.

	AUC	SE	95% CI	Sensitivity, %	Specificity, %
Diagnosis					
Histological/FCM	0.884	0.0247	0.840–0.920	83.33***	93.53***
Features					
Atypical glands	0.891	0.0239	0.840–0.926	83.82***	94.47***
Enlarged nuclei	0.930	0.0195	0.892–0.957	91.80***	94.17***
Prominent nucleoli	0.900	0.0230	0.857–0.933	92.86***	87.11***
Infiltrative pattern of glandular growth	0.891	0.0239	0.848–0.926	83.82***	94.47***

****P < 0.001.*

Fig. 2 Shows the different FCM findings in comparison to the histopathological evaluation; (**A** and **B**) shows the typical architecture of the prostate gland on FCM; (**C** and **D**) shows the architecture of the prostate gland on histopathological evaluation; (**E** and **F**) shows the atypical growth of the prostate gland and the enlarged nuclei with prominent nucleoli on FCM; (**G** and **H**) shows the same features on histopathological examination.

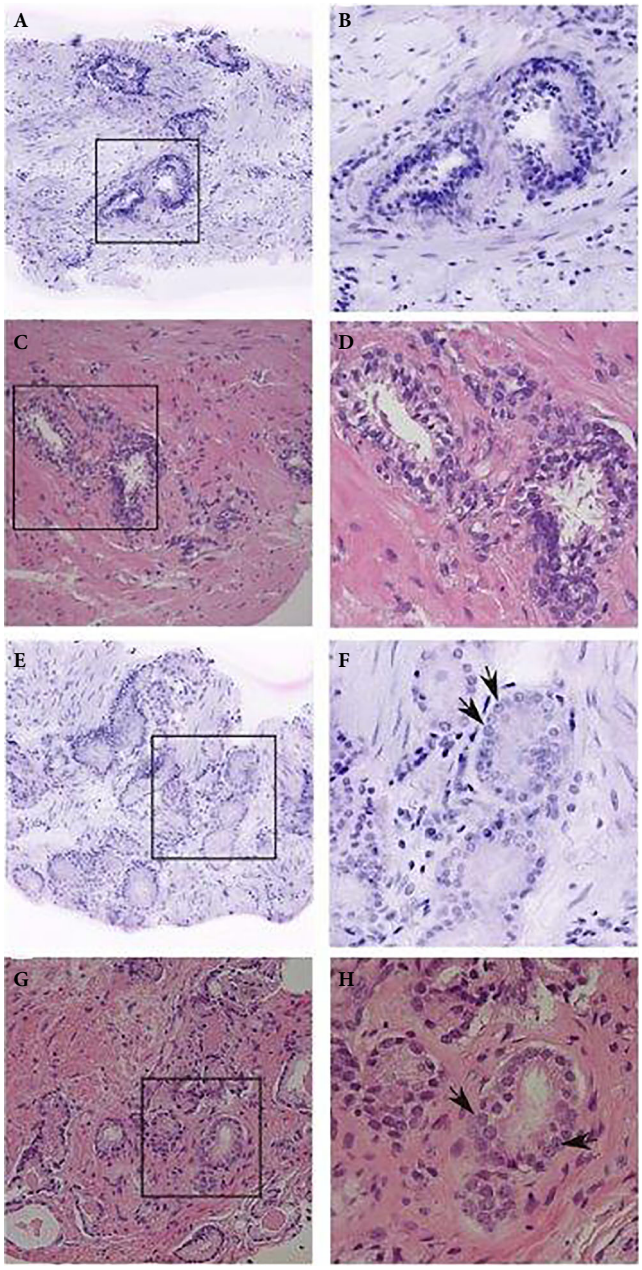

reproducibility. At ROC curve analysis, the enlarged nuclei had the highest AUC (0.930). The feature with the greatest sensitivity was prominent nuclei (92.86%) and the highest specificity was identified for atypical glands and the infiltrative pattern of glandular growth (94.47%). Figure 2 shows FCM digital images, including typical features of cancerous and non-neoplastic tissue, in comparison with corresponding histopathology images.

The pathologists' level of confidence with interpreting FCM digital imaging is reported in Fig. 3. According to the Pearson correlation coefficient, an overall positive correlation for all pathologists (0.536, $P < 0.001$) was observed (Table 3).

The inter-observer reliability, according to the ICC, was calculated to be 0.808 (95% CI 0.725–0.869) and 0.993 (95% CI 0.991–0.996) for FCM evaluation and histopathological diagnosis, respectively. This outcome reflects a good inter-observer reliability for FCM evaluation and an excellent reliability for histopathological examination.

Discussion

Our present preliminary experience with FCM, an optical microscopic tool that is able to analyse freshly excised specimens at histopathological-like resolution, suggests that prostate cancerous tissue and non-neoplastic tissue can be intraoperatively differentially diagnosed with a high reliability and reproducibility compared to histopathological diagnosis. This provides a base for future researchers to explore the potential application of this promising technology. FCM has been previously applied to different surgical settings, such as skin, breast, lymph node, thyroid, and colon [13], but has not previously been applied to prostate cancer.

A substantial level of agreement (κ-value = 0.75) between FCM and histopathological examination with an AUC of 0.884, an 83.3% sensitivity, 93.5% specificity and 91% accuracy compared to conventional histopathological evaluation was evidenced in the present preliminary cohort of prostate cancer samples. The neurovascular structure-adjacent frozen-section examination (NeuroSAFE) [8] is an established real-time approach, which has been proven to be a valid tool for intraoperative evaluation of periprostatic tissues. Its application on a series of 1040 patients with prostate cancer proved a significant improvement in the rate of nerve-sparing procedures (97% vs 81%) with a reduced PSM rate (16% vs 24%) compared to the non-NeuroSAFE group [22]. NeuroSAFE has a higher sensitivity, specificity and accuracy compared to the results of FCM in the present preliminary study (93.5%, 98.8%, and 97.3%, respectively) [8], but is more time consuming, requires a dedicated team of various specialists, and is more applicable to high-volume centres. Comparatively, FCM sample preparation can be performed by the treating surgeon and interpretation of digital images can be performed by a single pathologist, also via image transfer at an external location.

Another alternative real-time pathological analysis tool is confocal laser endomicroscopy (CLE). Cellvizio© (Mauna Kea Technologies, Paris, France) the most commonly used CLE

Fig. 3 Pearson correlation coefficient showing a positive correlation between the confidence of diagnosis and the gold standard (0.536, $P < 0.001$).

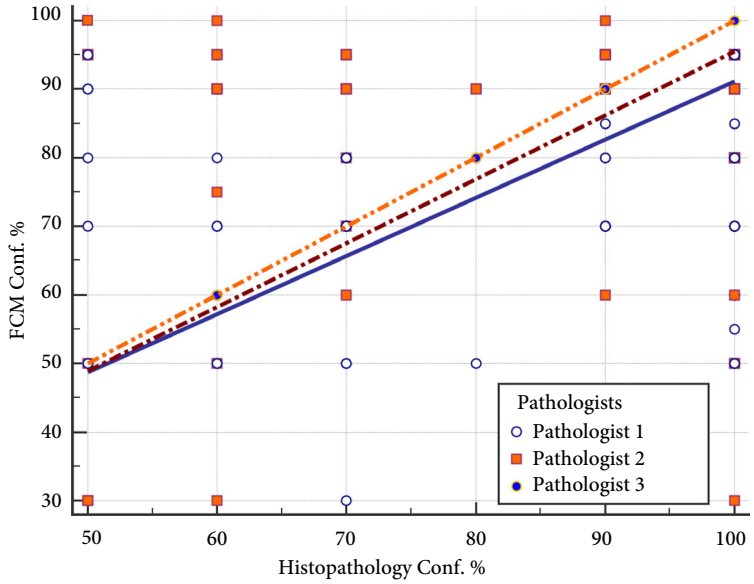

Table 3 Frequencies, κ-value, significance and reproducibility of prostatic adenocarcinoma features at FCM evaluation compared to histopathological evaluation for all pathologists.

	Features		Histological evaluation			Level of agreement	Reproducibility
			No	Yes	κ-value		
FCM evaluation	Atypical glands	No	188	11	0.78***	Substantial	Excellent
		Yes	11	57			
	Enlarged nuclei	No	188	11	0.78***	Substantial	Excellent
		Yes	11	57			
	Prominent nucleoli	No	196	29	0.64***	Substantial	Good
		Yes	3	39			
	Infiltrative pattern of glandular growth	No	194	12	0.83***	Almost perfect	Excellent
		YES	5	56			

*Frequencies, κ-value, significance and reproducibility of prostatic adenocarcinoma features at FCM evaluation compared to histopathological evaluation for all pathologists are illustrated. ***$P < 0.001$.*

system, has been applied to urology both during endourological procedures for TCC and during RP. Cellvizio consists of fibre optic probes for image acquisition, with a more shallow tissue penetration, a lower cell resolution and a smaller field of view, when compared to FCM [23]. However, it is worth mentioning that the NeuroSAFE and the Cellvizio were used to assess surgical margins, but in the present study random biopsies were taken from the prostate and the margins were not assessed, as our main aim was to initially assess the feasibility of FCM in prostatic tissue examination.

Other real-time pathological analysis of prostate cancer samples includes video-rate structured illumination microscopy (VR-SIM). VR-SIM is an *ex vivo*, wide-field optical sectioning technique, combining the use of 4.2 megapixel, high-speed scientific complementary metal-oxide semiconductor (CMOS) cameras and fast ferroelectric spatial light modulators for rapid pattern switching [24]. In a study of the pathological examination of 34 unfixed and uncut prostate cancer core biopsies, a similar AUC (0.82–0.88), and a lower sensitivity (62.5–87.5%), specificity (77.8–83.3%) and accuracy (76.5–82.4%) when compared to the present study were found [24].

Furthermore, multiphoton microscopy (MPM) has also been previously applied to prostate cancer in a descriptive study [25]. This imaging technology depends on the non-linear excitation caused by the simultaneous absorption of two or three low-energy photons, resulting in an internal optical sectioning resolution similar to FCM, but with superior tissue penetration. MPM was shown to be able to differentiate between benign and malignant prostatic tissues, but specificity and sensitivity analyses were not reported [25]. In the present study, FCM proved capable of not only differentiating between benign and malignant prostatic tissues, but was also able to identify specific histological features of prostate

cancer, with a substantial or almost perfect level of agreement compared to histopathological outcomes.

A simple and fast digital image acquisition with the requirement of a short learning curve (unpresented data) are amongst the main advantages of FCM compared to other currently available technologies (Cellvizio, VR-SIM, and MPM). The present study reports a high inter-observer reliability (ICC = 0.808) and a positive correlation between individual pathologist diagnostic confidence and histopathological diagnoses.

The intraoperative integration of FCM analysis may offer many advantages to the management of patients with prostate cancer, with a real-time simplified pathological analysis preparation and interpretation. Tissue management is extremely fast (<5 min) compared to VR-SIM (4–5 min) [24], Cellvizio (10 min) [23], NeuroSAFE (35 min) [8], and MPM (<60 min) [25]. Additionally, there are no fixation artefacts on the specimen and tissue integrity is maintained during FCM analyses, making the sample available for subsequent histopathological examination. However, these results should be interpreted with caution, as our present study did not assess the surgical margins.

Gleason Score is amongst the most important variables predicting the outcomes and prognosis of RP. Thus, the accurate reporting of the Gleason Score is crucial [26]. Interestingly, we tried to evaluate the ability of the FCM to differentiate between indolent prostate cancer (Gleason Sum ≤6) and clinically significant prostate cancer (Gleason Sum ≥7) showing 78% agreement between FCM and histopathology ($\kappa = 0.59$). However, this is just a preliminary result as it integrated only one of the three pathologists and it was not included in the aims of the present study (unpresented data). Currently, we have an ongoing study that includes the assessment of Gleason Score amongst its main endpoints.

Moreover, real-time differential identification between cancerous tissue and non-neoplastic tissue in prostate cancer surgery is essential but challenging. The reliability and reproducibility of this technology for the pathological examination of prostatic tissues reported in the present study represents the base upon which future researches can explore the benefits of this tool in the field of prostate cancer. In these settings, we are planning a new study to assess the use of the FCM in assessment of surgical margins during RALP.

The main limitation of our present study is the small sample size, which limits the robustness of our results. Moreover, the learning curve was not included in the aims of the present study. The surgical margin was not assessed in the present study, which is considered another limitation; however, this was intentionally done as we believe that the first step before using a new cellular imaging technology is to assess its feasibility and ability to differentiate malignant from benign characteristics and to ensure that it does not affect the integrity of the specimens. Further studies are required to confirm FCM diagnostic accuracy, create standardised FCM reporting and assess the associated learning curve on larger sample cohorts.

Conclusion

From our preliminary analysis, FCM seems to be a promising tool with a high reliability and reproducibility compared to gold standard diagnostics, offering rapid intraoperative evaluations with limited required personnel. Further studies are required to confirm these results and to explore the potential applications of this technology in urology.

Conflict of Interest

Ahmed Eissa has a temporary contract for 6 months as a urology consultant for MAVIG GmbH.

Funding

No funding was used for this study.

References

1 **Sooriakumaran P, Dev HS, Skarecky D, Ahlering T.** The importance of surgical margins in prostate cancer. *J Surg Oncol* 2016; 113: 310–15

2 **Palisaar RJ, Noldus J, Graefen M, Erbersdobler A, Haese A, Huland H.** Influence of nerve-sparing (NS) procedure during radical prostatectomy (RP) on margin status and biochemical failure. *Eur Urol* 2005; 47: 176–84

3 **Pasticier G, Rietbergen JB, Guillonneau B, Fromont G, Menon M, Vallancien G.** Robotically assisted laparoscopic radical prostatectomy: feasibility study in men. *Eur Urol* 2001; 40: 70–4

4 **Vourganti S, Rastinehad A, Yerram N et al.** Multiparametric magnetic resonance imaging and ultrasound fusion biopsy detect prostate cancer in patients with prior negative transrectal ultrasound biopsies. *J Urol* 2012; 188: 2152–7

5 **Mottet N, Bellmunt J, Bolla M et al.** EAU-ESTRO-SIOG guidelines on prostate cancer. Part 1: Screening, diagnosis, and local treatment with curative intent. *Eur Urol* 2017; 71:618–29.

6 **Wang M, Tulman DB, Sholl AB et al.** Gigapixel surface imaging of radical prostatectomy specimens for comprehensive detection of cancer-positive surgical margins using structured illumination microscopy. *Sci Rep* 2016; 6: 27419.

7 **Retèl VP, Bouchardy C, Usel M et al.** Determinants and effects of positive surgical margins after prostatectomy on prostate cancer mortality: a population-based study. *BMC Urol* 2014; 14: 86

8 **Schlomm T, Tennstedt P, Huxhold C et al.** Neurovascular structure-adjacent frozen-section examination (NeuroSAFE) increases nerve-sparing frequency and reduces positive surgical margins in open and robot-assisted laparoscopic radical prostatectomy: experience after 11,069 consecutive patients. *Eur Urol* 2012; 62: 333–40

9 **Gillitzer R, Thüroff C, Fandel T et al.** Intraoperative peripheral frozen sections do not significantly affect prognosis after nerve-sparing radical prostatectomy for prostate cancer. *BJU Int* 2011; 107: 755–9

10 **Gal AA.** In search of the origins of modern surgical pathology. *Adv Anat Pathol* 2001; 8: 1–13

11 **Longo C**, **Borsari S**, **Pampena R et al.** Basal cell carcinoma: the utility of in vivo and ex vivo confocal microscopy. *J Eur Acad Dermatol Venereol* 2018; 32: 2090–6

12 **Manfredini M**, **Longo C**, **Ferrari B et al.** Dermoscopic and reflectance confocal microscopy features of cutaneous squamous cell carcinoma. *J Eur Acad Dermatol Venereol* 2017; 31: 1828–33

13 **Ragazzi M**, **Piana S**, **Longo C et al.** Fluorescence confocal microscopy for pathologists. *Mod Pathol* 2014; 27:460–71.

14 **Bertoni L**, **Azzoni P**, **Reggiani C et al.** Ex vivo fluorescence confocal microscopy for intraoperative, real-time diagnosis of cutaneous inflammatory diseases: a preliminary study. *Exp Dermatol* 2018; 27: 1152–9

15 **Hartmann D**, **Krammer S**, **Ruini C**, **Ruzicka T**, **von Braunmuhl T**. Correlation of histological and ex-vivo confocal tumor thickness in malignant melanoma. *Lasers Med Sci* 2016; 31: 921–7

16 **MAVIG GmbH**. MAVIG VivaScope - Technical data [Internet]. Vivascope.de. 2019. Available at: http://www.vivascope.de/en/products/devices/ex-vivo-devices/vivascoper-2500-multilaser/technical-data.html. Accessed 14 February 2019

17 **Gareau DS**. The feasibility of digitally stained multimodal confocal mosaics to simulate histopathology. *J Biomed Optics* 2009; 14: 034050.

18 **Sprent P**, **Smeeton N**. *Applied Nonparametric Statistical Methods*, 4th edn. Boca Raton, IL: Chapman and Hall/CRC, 2007: 306–14

19 **Fleiss JL**. *The Measurement of Interrater Agreement, Statistical Methods for Rates and Proportions*, 2nd edn. NewYork: John Wiley, 1981: 212–36

20 **Koo TK**, **Li MY**. A guideline of selecting and reporting intraclass correlation coefficients for reliability research. *J Chiropr Med* 2016; 15: 155–63

21 **Epstein JI**, **Egevad L**, **Amin MB**, **Delahunt B**, **Srigley JR**, **Humphrey PA**. The 2014 international society of urological pathology (ISUP) consensus conference on Gleason grading of prostatic carcinoma: definition of grading patterns and proposal for a new grading system. *Am J Surg Pathol* 2016; 40:244–52

22 **Beyer B**, **Schlomm T**, **Tennstedt P et al.** A feasible and time-efficient adaptation of NeuroSAFE for da Vinci robot-assisted radical prostatectomy. *Eur Urol* 2014; 66: 138–44

23 **Lopez A**, **Zlatev DV**, **Mach KE et al.** Intraoperative optical biopsy during robotic assisted radical prostatectomy using confocal endomicroscopy. *J Urol* 2016; 195: 1110–17

24 **Wang M**, **Kimbrell HZ**, **Sholl AB et al.** High-resolution rapid diagnostic imaging of whole prostate biopsies using video-rate fluorescence structured illumination microscopy. *Cancer Res* 2015; 75: 4032–41

25 **Tewari AK**, **Shevchuk MM**, **Sterling J et al.** Multiphoton microscopy for structure identification in human prostate and periprostatic tissue: implications in prostate cancer surgery. *BJU Int* 2011; 108: 1421–9

26 **Mithal P**, **Howard LE**, **Aronson WJ et al.** Prostate-specific antigen level, stage or Gleason score: which is best for predicting outcomes after radical prostatectomy, and does it vary by the outcome being measured? Results from Shared Equal Access Regional Cancer Hospital database. *Int J Urol* 2015; 22: 362–6

Correspondence: Stefano Puliatti, Department of Urology, Ospedale Policlinico e Nuovo Ospedale Civile S. Agostino Estense Modena, University of Modena and Reggio Emilia, Modena, Italy.

e-mail: stefanopuliatti@gmail.com

Abbreviations: AUC, area under the curve; CLE, confocal laser endomicroscopy; FCM, fluorescence confocal microscopy; GGG, Gleason Grade Group; H&E, haematoxylin and eosin; ICC, interclass correlation; MPM, multiphoton microscopy; mpMRI, multiparametric MRI; NeuroSAFE, neurovascular structure-adjacent frozen-section examination; PSM, positive surgical margins; RALP, robot-assisted laparoscopic approach to RP; ROC, receiver operating characteristic; RP, radical prostatectomy; VR-SIM, video-rate structured illumination microscopy.